NEOPLASIA
www.neoplasia.com

Volume 22 Number 2 February 2020 pp. 61–75

Original Research

Long interspersed element-1 ribonucleoprotein particles protect telomeric ends in alternative lengthening of telomeres dependent cells

Thomas Aschacher[a]; Brigitte Wolf[b]; Olivia Aschacher[c]; Florian Enzmann[d]; Viktoria Laszlo[b]; Barbara Messner[a]; Adrian TÏrkcan[b]; Serge Weis[f]; Sabine Spiegl-Kreinecker[g]; Klaus Holzmann[e,h]; GÏnther Laufer[a]; Marek Ehrlich[a]; Michael Bergmann[b,h,*]

[a] Cardiac Surgery Research Laboratory, Department of Surgery, Medical University of Vienna, Waehringer Guertel 18-20, 1090 Vienna, Austria; [b] Surgical Research Laboratories, Department of Surgery, Medical University of Vienna, Waehringer Guertel 18-20, 1090 Vienna, Austria; [c] Department of Plastic and Reconstructive Surgery, Department of Surgery, Medical University of Vienna, Waehringer Guertel 18-20, 1090 Vienna, Austria [d] Department of Vascular and Endovascular Surgery, Paracelsus Medical University Salzburg, Muellner HauptstraÞe 48, 5020 Salzburg, Austria; [e] Department of Cancer Research, Borschkegasse 8a, 1090 Vienna, Austria; [f] Division of Neuropathology, Neuromed Campus, Kepler University Hospital, 4020 Linz, Austria; [g] University Clinic for Neurosurgery, Neuromed Campus, Kepler University Hospital, Johannes Kepler University, Linz, Austria; [h] Comprehensive Cancer Centre, Medical University of Vienna, Austria

Abstract

Malignant cells ensure telomere maintenance by the alternative lengthening of telomeres (ALT) in the absence of telomerase activity (TA). The retrotransposons ``long interspersed nuclear element-1'' (LINE-1, L1) are expressed in malignant cells and are primarily known to contribute to complex karyotypes. Here we demonstrate that LINE-1 ribonucleoprotein particles (L1-RNPs) expression is significantly higher in ALT$^+$- versus in TA$^+$-human glioma. Analyzing a role of L1-RNP in ALT, we show that L1-RNPs bind to telomeric repeat containing RNA (TERRA), which is critical for telomere stabilization and which is overexpressed in ALT$^+$ cells. In turn, L1-RNP knockdown (KD) abrogated the nuclear retention of TERRA, resulted in increased telomeric DNA damage, decreased cell growth and reduced expression of ALT characteristics such as c-circles and PML-bodies. L1-RNP KD also decreased the expression of Shelterin- and the ALT-regulating protein Topoisomerase IIIα (TopoIIIα) indicating a more general role of L1-RNPs in supporting telomeric integrity in ALT. Our findings suggest an impact of L1-RNP on telomere stability in ALT$^+$ dependent tumor cells. As L1-RNPs are rarely expressed in normal adult human tissue those elements might serve as a novel target for tumor ablative therapy.

Neoplastic (2020) 22 61–75

Keywords: Telomere, TERRA, LINE-1, DNA damage response, Alternative lengthening of telomeres

https://doi.org/10.1016/j.neo.2019.11.002
Received 28 June 2019; received in revised form 13 November 2019; accepted 14 November 2019

Abbreviations: ABP, ALT-associated PML bodies, ALT, alternative telomere lengthening, DDR, DNA damage response, GBM, Glioblastoma, hTERT, human telomerase reverse transcriptase, KD, knockdown, LINE-1/L1, long interspersed nuclear element-1, ORF, open reading frame, Poly(A), poly-adenylation, RNP, ribonucleoprotein, TA, telomerase activity, TBP, telomere binding proteins, TERRA, telomeric repeat containing RNA, TL, telomere length, TopoIIIα, Topoisomerase III-alpha, TSCE, telomeric sister chromatid exchange

* Corresponding author at: Surgical Research Laboratories, Division of General Surgery, Department of Surgery, Medical University of Vienna, Waehringer Guertel 18-20, 1090 Vienna, Austria.
e-mail address: michael.bergmann@meduniwien.ac.at (M. Bergmann), michael.bergmann@meduniwien.ac.at (M. Bergmann).

Introduction

Telomeres, heterochromatic nucleoprotein structures of repetitive DNA sequences (5′-TTAGGG-3′) and associated Shelterin proteins protect the ends of chromosomes from degradation and regulate cell survival [1–7]. Critical shortening of telomeres causes cell senescence and triggers apoptosis. Correspondingly, cancer cells reactivate TMM to ensure prolonged survival [2,8]. Usually malignant cells up-regulate telomerase, a reverse transcriptase that uses human telomerase-reverse transcriptase (hTERT) and an RNA template to add DNA repeats to the chromosomal ends [9–11]. In the absence of telomerase, tumor cells rely on the recombination-based alternative lengthening of telomeres (ALT) mechanism [12–14]. With respect to cancer development, ALT is predominantly observed in sarcomas, gliomas and neuroendocrine tumors [15–17]. ALT has been associated with mutations in the ATRX-gene coding for a chromatin remodeller. Depletion of ATRX or DAXX, both, which form a histone chaperone complex, lead to telomere dysfunction, which can be overcome by the recombination-based ALT mechanism [18,19]. Cells depending on ALT are characterized by high telomere length (TL) heterogeneity, ALT-associated PML bodies (APB), the occurrence of c-circles, and high levels of TERRA [12,16,20,21]. APBs seem to have an anchor function for telomeric ends as they build a protein cap around telomeric DNA. Those structures provide important supplements for telomere maintenance as they consist of Shelterin proteins as well as proteins involved in DNA damage repair (DDR) and homologous recombination [22]. Thus, APB appear to provide the ``recombinogenic microenvironment'', which is necessary to promote ALT TMM [23]. C-circles are extra-chromosomal telomeric DNAs in the form of single-stranded circular DNA that are present in ALT$^+$ cells and therefore count as markers for ALT [13]. To date their specific function remains speculative.

TERRA is thought to stabilize telomeres by delaying cellular senescence and sustaining genomic instability [24–28], and may regulate telomere maintenance [29]. Moreover, TERRA binds the telomeric c-strand to form RNA-DNA hybrids. As the RNAseH1 regulates the level of those hybrids, the appropriate amount of RNAseH1 ensures effective telomere maintenance in ALT [20].

ALT also relies on the generation of novel telomere sequences induced by double strand breaks due to replication fork collapse known as break induced replication (BIR). These novel telomere sequences are subsequently incorporated by intra- and inter-telomeric recombination [30]. The process of DNA branch migration and telomere synthesis involves POD3 and the BTR complex, the latter consists of BLM-TopoIIIα-hRMI$_{1/2}$, both found in the ABP complex. The BTR complex is needed to dissolve the recombination intermediates formed during strand invasion allowing telomeric extension [30,31]. This process is counteracted by the SLX4-SLX1-ERCC4 complex, which suppresses the branch migration and telomere synthesis leading to aborted telomeres. As TopoIIIα is part of the BTR complex, the depletion of TopoIIIα in ALT$^+$ cells result in a rapid accumulation of unresolved, post-replicative, recombination intermediates. This leads to abnormal mitosis and growth arrest [32]. ALT associated replication stress is regulated downstream by ATR and ChK1 and further involves the DNA translocase FANCM and BRCA1 [33]. FANCM forms an interaction with the BTR complex. The inhibition of the latter complex is toxic for ALT-dependent cells [34]. Thus, a better understanding of TMM regulation in ALT has the potential for novel therapeutic approaches in cancer therapy [35]. However, it is the mutual understanding, that multiple mechanisms promote ALT [36]. In this line, Zhang and colleagues recently found two distinct mechanisms of APB-associated break-induced DNA replication (BIR) in ALT. One pathway, RAD52 dependent does not lead to c-circles whereas the RAD52 independent pathway results in c-circle formation [23]. This finding might have therapeutic implication as deleting RAD52 and SLX4 have increased toxicity in ALT cells as either approach alone [37]. Thus, effective inhibition of ALT might require the understanding and targeting of multiple pathways [38].

LINE-1 encodes well known self-propagating retrotransposons and comprises 17% of the human genome [39]. A majority of LINE-1 sequences are inactive by containing non-functional open reading frames (ORFs). Only a small fraction of 5–8 L1-RNP elements are highly active [39]. A full length L1-RNP retrotransposon is ∼6 kb long and contains two open reading frames (ORFs) [39]. L1-ORF1 encodes a protein (L1-ORF1p) with RNA binding and nucleic acid chaperone activity, while L1-ORF2 encodes a protein (L1-ORF2p) with endonuclease and reverse transcriptase activity [40–44]. Physiological expression of LINE-1 was observed in embryogenesis, neuronal progenitor cells and germ line cells [45]. Week expression was found in heart, skin and thyroid [46] Disease associated reactivation has been reported in most of the cancer types [45,47–49]. Due to their ability to perform retrotransposition, active LINE-1 sequences are primarily thought to contribute to evolution influencing the genotype by genomic rearrangement. During development of cancer they promote complex cancer-associated karyotypes [50,51].

With respect to oncology we have found that LINE-1 reactivation appears to be an essential factor for TMM in TA$^+$ cells [50,51]. This further explains a reduced tumor cell growth upon LINE-1 inhibition *in vitro* and *in vivo* [51–53]. In this study, we show that a reduction of L1-RNPs is associated with telomeric damage in ALT-dependent cells.

Material and Methods

Human glioblastoma (GBM) tumor samples and patient characteristics

Nineteen GBM specimens (n = 19) were included in this study. All of the GBMs were operated at the Department of Neurosurgery, Neuromed Campus, Kepler University Hospital, Linz, Austria. For the current research project, the Division of Neuropathology at the Neuromed Campus provided the paraffin sections. Clinical information was obtained with written informed consent of all patients and the local ethics committee approved the study.

Cell culture

Cell lines SW-480, SW-620, HCT-116, SaOS-2, U-2OS (obtained from ATCC, Wesel, Germany) and the cell lines MG-63, GM-847 SV40-immortalized skin fibroblasts, WI38-VA13/2RA SV40-immortalized WI38 normal lung fibroblasts, G-292 osteosarcoma and the IIICF/c (ras) cell line were provided by R. Reddel (Children Medical Research Institute, Sydney, Australia). Cell lines were maintained in Dulbeccos modified Eagles medium (DMEM, Gibco Fisher Scientific, Austria) or McCoy's 5a (McCoy¨s 5a MOD with stable Glutamine, GIBCO, 26600-023, Fisher Scientific, Austria) supplemented with 10% fetal bovine serum (FBS, Gibco, Fisher Scientific, Austria). Primary human fibroblasts (HF + 400, provided by Christine Brostjan, Medical University of Vienna, Austria), were maintained in DMEM supplemented with L-Glutamin, sodium-pyrovate, gentamicin and amphotericin (Sigma-Aldrich, Vienna, Austria). Applied-Genetics (Eurofins Medigenomix-GmbH, Ebersberg, Germany) and Fragment-Analysis-Facility (John Hopkins University, Baltimore, MD) provided cell line quality control.

siRNA transfection

The L1-RNP-targeted siRNA oligonucleotides and the scrambled siRNA were designed to target the active L1-RNP elements (predesigned and validated from Invitrogen). siRNA/lipid solutions were prepared with Lipofectamine 2000 (Invitrogen, Fisher Scientific, Austria) and

36 pmol of siRNAs. For siRNA transfection using the standard method was prepared followed by manufactorys instruction (Invitrogen, Fisher Scientific, Austria). The sequences of siRNA were: scrambled-siRNA 5′-GAA GAAGGAGCGGAAGAAGUUAUUA-3′; L1-RNP-siRNA #1288 GAA AUGAAGCGAGAAGGGAAGUUUA, L1-RNP-siRNA #1264 TCAG CAATGGAA GATGAAATGAATG, L1-RNP-siRNA 1329 AAGAAAT GAGCAAAGCCTCCAAGAA. To target the TopoIIIα cDNA sequence (NM004618), we used the previously described siRNA sequence 5′-CCA GAAAUCUUCCACAGAA-3′ [32].

RNA isolation and real-time PCR (RT-qPCR)

RNA was isolated using Trizol (PeqGOLD TriFast, Peqlab, VWR, Vienna, Austria) followed by purification with the E.Z.N.A. Microelute Total RNA Kit (Omega Bio-Tek, VWR, Vienna, Austria), including the optional DNA digestion step (RNase-free DNase I Set, Omega Bio-Tek, VWR, Vienna, Austria). After quantification equal amounts of total RNA were reverse-transcribed using the QuantiTect Reverse Transcription Kit (Qiagen, Hilden, Germany). For RT-qPCR, cDNA and gene specific primers were used with the Maxima® SYBR Green/ROX RT-qPCR MM (2X) (Fermentas Fisher Scientific, Austria) or the GoTaq RT-qPCR Master Mix (Promega, Mannheim, Germany). Samples were normalized to the geometric mean of two reference genes (gapdh, rplp0). Oligonucleotide primer sequences were: L1-RNP-ORF1_fwd-AGGAAA GCCCATCAGACTAACAG; L1-RNP-ORF1_rev-GGCCTGGTGGT GACAAAATCT; L1-RNP ORF2-s-GAAATGGATACATTCCTCGA CACA; L1-RNP-ORF2-as-CTGGTCCTGGACTCTTTTTGGT; GA PDH_f-TGCACCACCAACTGCTTAGC; GAPDH_r-GGCATGGAC TG TGGTCATGAG; RPLP0_f-AGCCCAGAACACTGGTCTC; and RPLP0_r-ACTCAGGATTTCAATGGTGCC; APOBEC3C_f-GCATA TCTAAGAGGCTGAACATGAAT; APOBEC3C_r-TGGAAGTAGAA TGTGCCTGGATAC; APOBEC3H_f-CAGCTGACGCCGCAGAA T; APOBEC3H_r-GACTTGATCTCGTTAATAAAGCAAATTTC; AP OBEC3G_f-GTGGAGCGCATGCACAATG; APOBEC3G_r-GGCCT TCAAGGAAACCGTGT; ACTB_f- AGGCACCAGGGCGTGAT; ACTB_r-TGTAGAAGGTGTGGTGCCAGATT; TOP3A_f-GCATC GACTCTTTAACCACACGG; or TOP3A_r-CTCCACAGTGTTCC AAGGCTTGA.

Telomeric length and TERRA measurements by RT-qPCR

The average telomere length ratio was measured from total genomic DNA or cDNA as previously described [54].

Telomere length measurement

For PFGE/Southern blot, agarose plugs containing 25,000 cells were prepared, for protein digestions plugs were incubated with 0.5 mg/ml Proteinase K (Roche, Sigma-Aldrich, Vienna, Austria) at 50 °C for 24 h. Digested plugs were inserted into an 1% pulsed-field agarose gel and electrophoresed for 20 h at 12 °C with logarithmic interval decay in a Chef DR III apparatus (Bio-Rad, Vienna, Austria). Electrophoresis settings were as follows, block 1: 3 h, interval 20–10 s, 4 V/cm, angle 120°; block 2: 8 h, interval 10–5 s, 5 V/cm, angle 120°; block 3: 5–2 s, 4 V/cm, angle 110°. Electrophoretically separated DNA fragments were vacuum-blotted onto a positively-charged nylon membrane (Roche, Sigma-Aldrich, Vienna, Austria) with a VacuGene XL apparatus (GE Healthcare, Vienna, Austria), applying a depurination (0.25 N HCl for 30 min), denaturation (0.5 M NaOH, 1.5 M NaCl, 30 min), neutralization (0.5 M Tris-HCl, 3 M NaCl, pH 7.5, 30 min) and blotting (3 M NaCl, 0.3 M Na-citrate, pH 7, 2 h) step. Detection of telomere fragments was done with the Telo TAGGG Telomere length assay (Roche, Sigma-Aldrich, Vienna, Austria) according to the manufacturer's instructions. For telomere length measurements in GBM tumors, the telomere lengths were measured by a qPCR approach as published in LÎtsch et al. [55]. DNA from the osteosarcoma cell line Sa-OS positive for the alternative lengthening of telomere (ALT) mechanism was used as long telomere control. Telomere lengths of all samples analyzed were given in relation to SaOS-2 set arbitrarily as 1.

Immunoblot

Cells were scraped from cell-culture plates, washed in ice-cold PBS and lysed in M-PER™ Mammalian Protein Extraction Reagent containing 1x Halt protease inhibitor cocktail (ThermoFisher Scientific, Vienna, Austria). Protein extracts were quantified with the BCA Protein Assay Kit (Pierce, ThermoFisher Scientific, Vienna, Austria). 30 µg of protein was denatured with Laemmli buffer, loaded into each well of an 8% acrylamide-bisacrylamide (37.5:1) gel containing 0.1% SDS and electrophoresed with 25 mA/gel for 150 Vh. Proteins were transferred to a PVDF membrane using the Transblot Turbo and the RTA Ready-to-assemble Transfer Kit (Bio-Rad, Vienna, Austria). After several hours of blocking PVDF membranes were incubated with the primary antibodies as indicated in 5% NFDM/TBS-T for 1 h at room temperature. After washing with TBS-T membranes were incubated with the secondary antibody anti-rabbit IgG HRP linked Antibody (Cell Signaling, Cat. 7074S, 1:5000, 1 h, room temperature). Detection was done with ECL Ultra Western Blotting HRP Substrate (Lumigen, Inc.) for LINE-1 or ClarityTM Western ECL Substrate (Bio-Rad, Vienna, Austria) for β-Tubulin. Protein band intensities were quantified with ImageQuant TL 7.0 (GE Healthcare, Vienna, Austria).

Immunofluorescence microscopy

For immunofluorescence staining cells were seeded on 13 mm coverslips and fixed with formaldehyde (prepared from paraformaldehyde) for 15 min at room temperature or with ice-cold methanol for 10 min at −20 °C in case of Line-1 staining. After permeabilization with 0.2% TritonX-100 in TBS and blocking (10% goat serum, 1% BSA, 0.05% Tween20, 0.3 M glycin in TBS), coverslips were incubated with the primary antibodies as indicated in 1% BSA in TBS over night at 4 °C. After washing with TBS-T slides were incubated with 1:400 diluted secondary antibodies in 1%BSA/TBS for 1hr at room temperature: Goat anti-Rabbit IgG (H + L) Secondary Antibody, Alexa Fluor 546 or Goat anti-Mouse IgG (H + L) Secondary Antibody, Alexa Fluor 488 (molecular probes, ThermoFisher Scientific, Vienna, Austria). DNA were counterstained with DAPI (ThermoFisher Scientific, Vienna, Austria). Microscopy pictures were taken on a Confocal Laser Scanning Microscope 700 with a 63x/ 1.4 plan-apochromat, Oil, DIC objective (Zeiss, Vienna, Austria). For spot counting and co-localization analysis images were analyzed with the CellProfiler™ cell image analysis software [56]. For ABP measurements in GBM specimens, indirect immunofluorescence was performed using the anti-PML mouse monoclonal antibody conjugated to Alexa Fluor 488. Telomere fluorescence in situ hybridization was done with the Telomere PNA FISH kit/Cy3 according to manufacturer's instructions. (Dako, Denmark).

Antibodies

Primary antibodies were TRF-2 (SantaCruz H-300, sc-9143, rabbit polyclonal, 20 µg/ml), γH2AX (Abcam, Anti-gamma H2A.X (phospho S139 antibody [9F3], ab26350, mouse monoclonal, 10 µg/ml), PML (PG-M3, SantaCruz, sc-966, mouse monoclonal, 2 µg/ml), anti-TRF1 (Abcam, TRF-78, ab10579), TIN2 (Abcam, ab197894), POT1 (Abcam, ab90552),

RAP1 (Abcam, ab40144), ATRX (Abcam, ab97508), TopoIIIα (SantaCruz, sc13060, rabbit polyclonal), DAXX (Abcam, ab32140), LINE-1 (SantaCruz H110, sc67197, rabbit polyclonal), LINE-1 (chA1-L1-RNP, mouse monoclonal, 40 µg/ml) [46], or β-Tubulin (9F3) rabbit IgG mAb (Cell Signaling, Cat. # 2128S, 1:10000, overnight, 4 °C), Anti-p21 antibody [EPR18021] (Abcam, ab188224), hTERT-antibody (Abcam, ab183105), Anti-Caspase-3 (Abcam, ab13847).

Anaphase-bridge formation

Tumor cell lines were treated, fixed and permeabilized as described above. For the nuclear staining, DNA were mounted in Vectashield mounting medium with 0.5 µg/ml DAPI (VectorLabs, Maravai LifeSciences, CA, USA) and detected as described for immunofluorescence microscopy.

Q-Fish

Q-Fish analyses were done as previously described[3]. Briefly, indicated cells were fixed with 3.7% formaldehyde, treated with Pepsin (Sigma Aldrich, Vienna, Austria), and dehydrated. Followed by hybridization with PNA-FITC-$(CCCTAA)_4$ probe dissolved in a hybridization buffer (70% formamide, 2 µg/µl BSA, 10% dextran sulfate in 2xSSC) O/N. Next day, cells were washed three times in 2xSSC, 70% formamide at 39 °C, and 3 times in PBS. Slides were dehydrated and mounted in Vectashield mounting medium with DAPI (VectorLabs, Maravai LifeSciences, CA, USA).

Telomeric RNA FISH

RNA Fish was performed as described [28], except that a PNA-FITC-$(CCCTAA)_4$ probe dissolved in a hybridization buffer (70% formamide, 2 µg/µl BSA, 10% dextran sulfate in 2xSSC) was used for visualization of TERRA(UUAGGG)-repeats. 48 h after transfection cells were incubated for 7 minutes in ice-cold freshly made CSK buffer (100 mM NaCl, 300 mM sucrose, 3 mM $MgCl_2$, 10 mM PIPES pH 7, 0.5% Triton-X100) containing 40U/ml SUPERase.In. Cells were then fixed with 4% paraformaldehyde and rinsed with 70% EtOH, air-dried and hybridization was performed overnight at 37 °C. Slides were then washed 3 times in 2xSSC, 70% formamide at 39 °C, and 2 times in 2xSSC. Slides were dehydrated and mounted in Vectashield mounting medium with DAPI (VectorLabs, Maravai LifeSciences, CA, USA).

Cell cycle and cell death analyses

Cell cycle and annexin V-staining were done as previously described [57]. Measurements and calculations were performed by flow cytometer MultiCycle AV software, Version 6.0 (Phoenix Flow Systems Inc., San Diego, CA).

Chromatin immunoprecipitation (ChIP), RNA-Immunoprecipitation (RIP) and telomere-specific dot blots

DNA-ChIP and RIP were prepared followed by manufacturer's instruction (Abcam). Chromatin bound fractions were immunoprecipitated with indicated antibody O/N at 4 °C, followed by incubation with cleared Protein A/G-beads, reverse crosslinking and the DNA was eluted. The immunoprecipitated DNA was quantified by using quantitative PCR and run on 1.5% agarose gels. The sequences of the primers used in this study were previously described [54]. For telomeric dot blots, eluates were dot blotted onto Hybond N^+ membrane (GE Healthcare, Buckinghamshire, UK). For RIP, cells were lysed in 1XCHAPS buffer with the addition of protease inhibitor cocktail and SUPERase.In (40U/ml), sonicated and clarified by centrifugation, pre-cleared with A/G beads (Santa Cruz, Heidelberg, Germany) and immunoprecipitated with indicated antibodies O/N at 4 °C. On the next day, agarose A/G beads were added and rotated for 2 h at 4 °C. RNA and proteins were extracted using Trizol reagents and dot blotted onto Hybond N^+ membrane. Telomeric DNA or RNA was detected with the TeloTAGGG telomere length assay kit (Roche LifeScience, Vienna, Austria) using C-rich strand $(CCCTAA)_6$ or G-rich strand $(TTAGGG)_6$, and visualized by Typhoon Scanner (MolecularDynamics, Harlow Scientific, MA).

C-circle assay

For the C-circle assay, DNA from cell lines was isolated by salting-out and quantified using the QuantiFluor dsDNA System (Promega, Mannheim, Germany) on a Varioskan Flash plate reader (ThermoFisher Scientific, Austria). The assay was performed using 20 ng DNA as described by Henson et al. 2017. Briefly, the circular fraction from genomic DNA was amplified by rolling circle amplification with Φ29 DNA polymerase. Amplification products were dot-blotted onto nylon membranes and hybridized with a digoxigenin-labeled telomeric oligonucleotide probe $[AATCCC]_4$. Digoxigenin was detected with an alkaline-phosphatase coupled anti-digoxigenin antibody [58].

RNA ligation and RNA/DNA electrophoretic mobility shift assay (EMSA)

RNA was labeled with 3′End Biotinylation Kit (Pierce Chemical, Rockford, IL). Gel shift analysis was performed as previously described [59]. Briefly, proteins were incubated with 50 pM biotin-labeled RNA probes (poly(A)$^+$TERRA G-$(UUAGGG)_4$-$UU(A)_{18}$; poly(A)$^-$ TERRAAGGG-$(UUAGGG)_7$) or DIG-labeled telomeric DNA probes (C-strand: DIG-$(CCCTAA)_6$ and G-strand: DIG-$(TTAGGG)_6$) in EMSA buffer [50 mM KCl, 5% (vol/vol) glycerol, 0.1% (vol/vol) NP-40, 1 mM MgCl2, 5 mM dithiothreitol, 10 mM Tris-HCl, pH 8.0], with (for supershift) or without L1-RNP-antibody (LINE-1H-110, Santa Cruz) pre-incubation for 10 minutes, followed by incubation for 20–60 min at RT. The samples were run on a 10% native acrylamide gel and transferred to positive-charge nylon membrane. The signals were detected by LightShift chemiluminescent kit (Pierce Chemical, Rockford, IL).

Plasmids and expression of purified L1-RNP

Two plasmids, pLD24 and pLD48 expressing synthetic human L1-RNP-ORF1 and L1-RNP-RT, respectively were kindly provided by Jeff D. Boeke (Department of Molecular Biology and Genetics, Johns Hopkins University School of Medicine, Baltimore). Expression and purification of the two plasmids were done as previously described [60].

In-vitro reverse-transcriptase assays

L1-RNP-specific telomeric RT-assay (t-RTA) was done as previously described with minor changes [60,61]. For the RT-assay, cell lysates were extracted with CHAPS lyses buffer and RT-assays were performed in a 20 µl reaction (2 µg protein). As negative control, lysates were treated with RNaseA (100 µg/ml) for 20 min at 37 °C. t-RTA reaction buffer containing 50 mM Tris-Cl (pH 8.0), 5 mM MgCl2, 50 mM KCl, 10 mM DDT, 0.05% Triton-X100, 2 mg/ml BSA, 2.5 µM dNTPs, and with indicated primer (Oligo(T) [16,21,22] or sequence as described for insertion and elongation assay) at 37 °C for 2 h min followed by RNaseA (100 µg/ml) and proteinaseK (50 µg/ml) treatment, and heated up to 98 °C for

10 min. RTA-reactions were spotted onto Hybond N^+ membrane. C-strand or G-strand specificity was visualized by telomeric dot blotting (as described above).

Statistical analysis

A one-tailed student's t-test (for comparison of cell line differential values) or Mann-Whitney tests were used for statistical comparisons where appropriate. A two-sided *p value* below 0.05 was considered significant. Statistical analysis was performed with GraphPad Prism software package (Version 4; GraphPad Software, Inc., La Jolla, CA, USA) and SPSS (IBM SPSS Statistics). Error bars represent s.e.m. or s.d., as indicated in the figure legends. All experiments were performed three or more times independently under identical or similar conditions, except when indicated in the figure legends.

Results

Association of L1-RNP-expression and ALT in human tumor

In order to investigate a potential correlation of L1-RNP expression and ALT mechanism in human cancer, we compared L1-RNP expression in ALT^+/TA^- versus TA^+ in glioblastoma (GBM), WHO grade IV. This tumor entity is characterized by the occurrence of ALT^+ and TA^+ tumors allowing comparative studies. The ALT^+/TA^- phenotype in our GBM specimens was characterized by significantly longer telomeres, positive staining for ABPs, the lack of hTERT mRNA expression, and negative TRAP assay compared to the TA^+ phenotype (Fig. 1A–C and Supplementary Table). In accordance to the literature the ALT^+/TA^- revealed a significant reduction of ATRX protein levels as compared to TA^+ samples ($p = 0.03$) (Supplementary Fig. 1). We only observe a tendency but not a significant difference in DAXX protein levels in the two groups ($p = 0.06$).

L1-RNP expression was significantly increased in tumor specimens of the ALT^+/TA^- phenotype compared to tumor of the TA^+ phenotype (Fig. 1, *D and E*). This clinical observation suggests a specific association of higher L1-RNP-expression in human ALT^+ tumors compared to TA^+ tumors.

L1-RNP knockdown in ALT⁺ tumor cells lead to telomere-dysfunction

As we observed a high L1-RNP expression in ALT^+ glioma, we next investigated whether L1-RNP expression had an influence on telomere stability in ALT^+ cell lines. RNAi-mediated reduction of functional L1-RNP (L1-KD) was performed in the ALT^+ cell lines as previously described [51] leading to a reduction of ORF1- and ORF2-mRNA expression as well as reduced L1-RNP protein expression (Fig. 2A and Supplementary Fig. 2). Correspondingly to recent findings [62] L1-RNP expression was also time-dependent in our cell lines. Increased L1-RNP expression could not be assigned to a certain type of TMM in vitro (Supplementary Fig. 3). We first analyzed the influence of L1-KD on DNA strand breaks located on telomeres known as TIF [63]. TIFs were detected by co-localisation of DDR signals, by using an γH2AX-specific antibody and TRF-1/2 signals. We observed a significant increase of TIFs in ALT^+ tumor cells treated with L1-RNP-siRNA compared to scrambled-siRNA treatment within 24–48 h post-transfection (Fig. 2, *B and C*). This effect was restored after 72–96 h post-transfection (data not shown). Strand breaks at telomeres can lead to chromosome fusion followed by formation of anaphase bridges [63,64]. L1-KD with siRNA led to a significant increase in the number of anaphase-bridges in ALT^+ tumor cells (Fig. 2, *D and E,* Supplementary Fig. 4).

A consequence of DNA damage and chromosomal instability are micronuclei formed during anaphase. Correspondingly, we detected an increase in micronuclei in ALT^+ cell lines treated with L1-RNP-siRNA as compared to scrambled-siRNA (Fig. 2, *F and G*). These observations confirmed that a reduction of L1-RNP expression increased DNA damage and chromosomal integrity on telomeres. Therefore, we analyzed a potential association of L1-RNP and telomere binding proteins (TBP), which are essential for telomere stability. A decrease of L1-RNP was associated with a reduced TRF-1 and TRF-2-protein and -mRNA expression in ALT^+ cells (Fig. 2H and Supplementary Fig. 5).

We also determined the TL of ALT^+ tumor cells by the terminal restriction fragment assay, 24, 48 and 72 h after L1-RNP-siRNA treatment. A reduction of L1-RNP was associated with a non-significant shortening of TL (data not shown). Due to the very long telomeres in ALT^+ cells a non-significant reduction in size might not rule out a contribution of L1-RNP to telomere regulation within 3 days of siRNA treatment.

A decrease of L1-RNP shows cellular growth impairment in ALT^+ tumor cells

In TA^+ cells, we observed a correlation of L1-KD-induced telomere dysfunction and a cell cycle arrest followed by a reduced growth rate [51]. Similarly, L1-KD in ALT^+ cell lines led to a pronounced cell cycle arrest in G2/M phase, which was paralleled by a significant impairment of cell growth (Fig. 3, *A and B*). L1-KD induced a significant increase in apoptosis in ALT^+ tumor cells when compared to controls (Supplementary Fig. 6).

Corresponding to annexin V and cell cycle analysis, we found caspase 3 activation after L1-KD shown in ALT^+ cell lines measured by Western

Fig. 1. L1-RNP is overexpressed in human glioblastoma (GBM) (Who grade IV) with impact on telomere maintenance mechanism in these tumors. A, The ALT^+ phenotype in GBM specimens was correlated with significantly longer telomeres measured by Southern blot. Mean TRF of telomeres is given for TA+ (red) and ALT+ (blue) tumors. TMM were verified by hTERT mRNA expression and telomerase activity measurements. B, Telomerase activity (TA) in GBM analyzed by the telomeric repeat amplification (TRAP) assay. Representative examples for TA pos. and TA neg. tumor samples from patients 12, 14, 3 and 9 are depicted. M, 20 bp marker; NTC, no template control; IS, internal standard; TSR8, quantitation control template. For each sample (500 ng protein extract), the TRAP assay was performed with (+) and without (−) heat treatment. C, Representative image of ALT-associated PML bodies (APBs) analysis in GBM. Combined PML immunofluorescence and telomere fluorescence in situ hybridization in a GBM derived prim-cell culture representative for ALT (Patient 3). Cytospin preparations were analyzed with a 100× objective. Overlap of the PML (green) and telomeric foci (red) indicate the presence of APB (yellow). Scale bar, 100 µm. D, Association of high L1-RNP expression in ALT^+ GBM samples. ICC staining against L1-RNP-ORF2 was done to reveal the L1-RNP protein status in GBM specimens. Two different L1-RNP antibodies (please find Material & Methods) were used in separate staining experiments. Representative images of one series are given for TA^+ and ALT^+ tumors. Cell nuclei DNA were stained with PI (red signal); L1-RNP (green signal). Enlargement of L1-signals in ALT^+ tumor group is shown. E, Diagram shows mean fluorescence intensity of L1-RNP staining in GBM. Difference between both groups is statistically significant ($p < 0.001$). Data shown are representative of two independent ICC staining.

Blot (Fig. 3C). Caspase 3 is involved in the activation cascade of caspases responsible for apoptosis execution [65]. We further analyzed *p*21 protein in ALT$^+$ cells after L1-KD. Protein *p*21 binds to and inhibits cyclin-dependent kinase activity, preventing phosphorylation of critical cyclin-dependent kinase substrates and blocking cell cycle progression [65]. We observed a decrease of *p*21 protein in cells after L1-KD as compared to n.i.-treated cells as determined by Western Blot analysis (Fig. 3D).

The APOBEC3 (A3) superfamily (including A3C, A3D and A3H) proteins play important roles in antiviral immunity related to retroviruses, retroviral elements and RNA editing enzymes that involve RT-activity regulation, but also in tumor cell growth and cell cycle control [66–69]. Concerning retrotransposons, hypomethylation of L1-RNP genomic copies was shown to be associated with increased APOBEC-mRNA expression. Correspondingly, we found that L1-KD resulted in a decrease of mRNA expression of A3-superfamily proteins A3C, A3D, and A3H in ALT$^+$ tumor cells (Fig. 3E). Thus, L1-KD induced cell cycle arrest correlated with a decrease of mRNA of the cell cycle promoting APOBEC proteins.

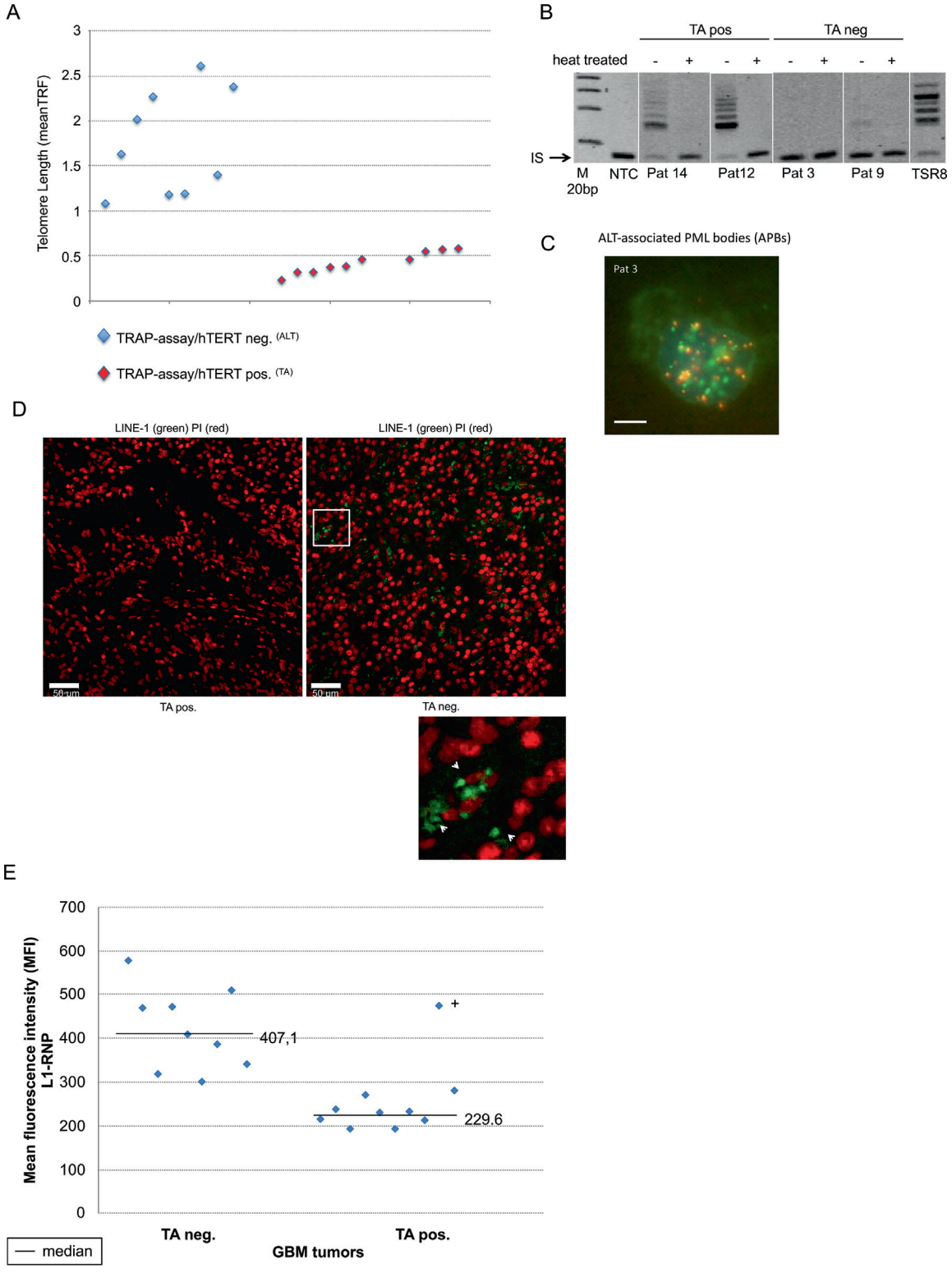

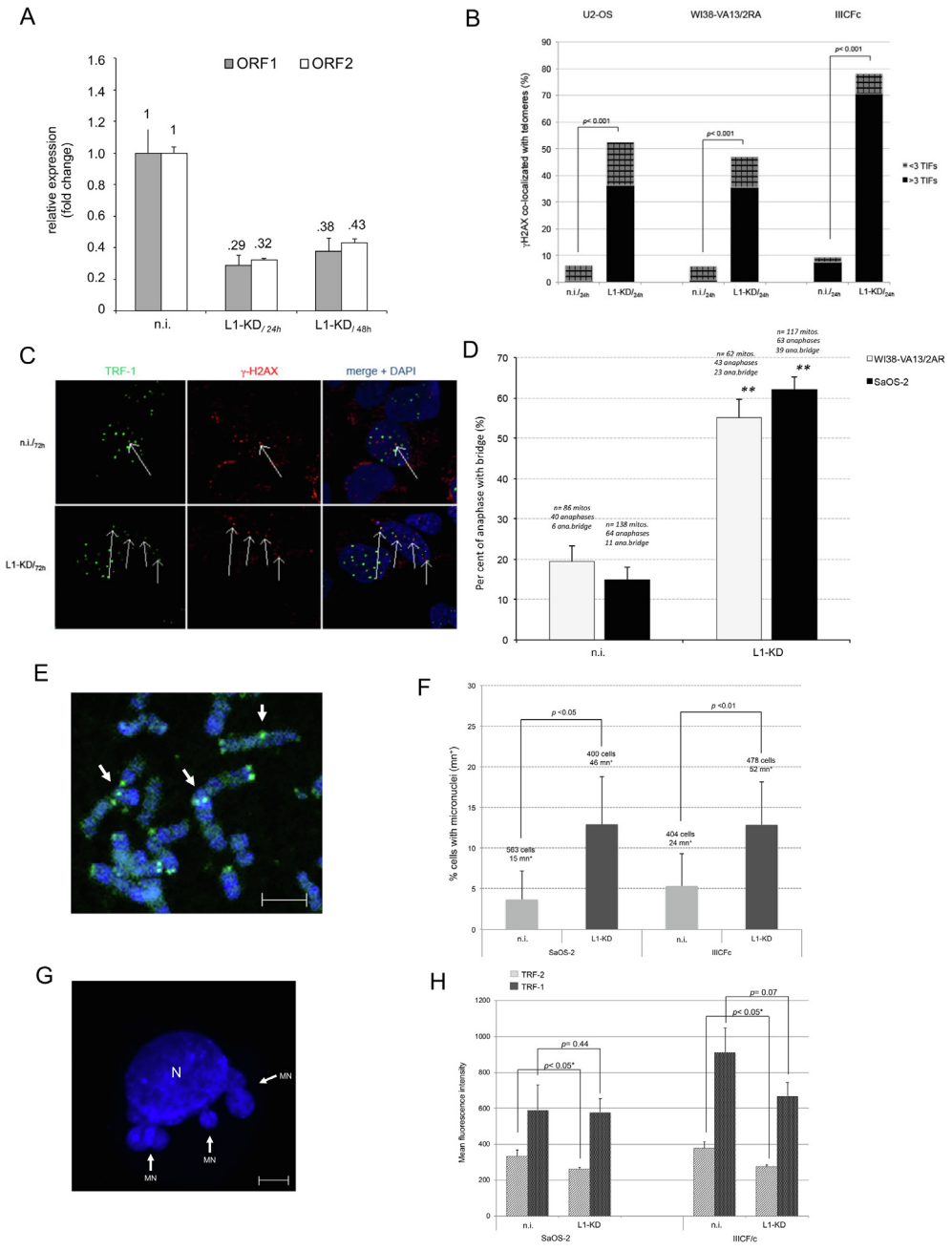

Fig. 2. L1-RNP knockdown leads to a decrease of telomere stability. A, Representative images showing the L1-RNP expression in ALT$^+$ cell line SaOS-2 treated with non-interfering siRNA (n.i.) and siRNA targeting L1-RNP (L1-KD) determined by RT-qPCR statistic. B, C, L1-KD is associated with telomeric induced foci (TIFs). Statistical comparison of ALT cell lines is given (B). Cell lines used as indicated on the top. Gray bar: 1–3 TIFs; black bar: >3 TIFs. n = 3. error bars are s.d. Representative image of telomeric induced foci (C). red, γH2AX; green, telomeres. Arrows indicate co-localization. D, E, L1-KD is associated with an increase in anaphase bridges. The frequency of anaphase bridges in ALT cells was calculated as the ratio between cells exhibiting anaphase bridges and the total number of anaphase cells (D). Cell lines and treatment as indicated. n = 4 **) $p < 0.01$; error bars are s.d. A representative image of telomeric DNA Q-FISH is shown (E). Green spots are indicating telomeric ends and arrows the telomere fusion of two chromosome ends (blue, DNA staining). F, G, Increased number of micronuclei next to the nucleus were observed 5 days after L1-RNP-siRNA transfection, compared to scrambled non-interfering (n.i.) siRNA. Diagram of cells positive for micronuclei are shown (F). Cell counts, micronuclei positive (mn$^+$) nuclei, statistical significance and cell lines as indicated. n = 3. Representative image with positive micronuclei (MN) next to the nucleus (N) is shown (G). H,I, Inhibition of L1-RNP reduced TRF-1 and TRF-2 proteins measured by Western blot in SaOS-2 cell line (representative image is shown, (H) and ICC staining (I). cell lines, statistical significance and treatment as indicated. n = 3. All statistical data shown are representative of three independent experiments; error bars are s.d. blue, DNA-staining.

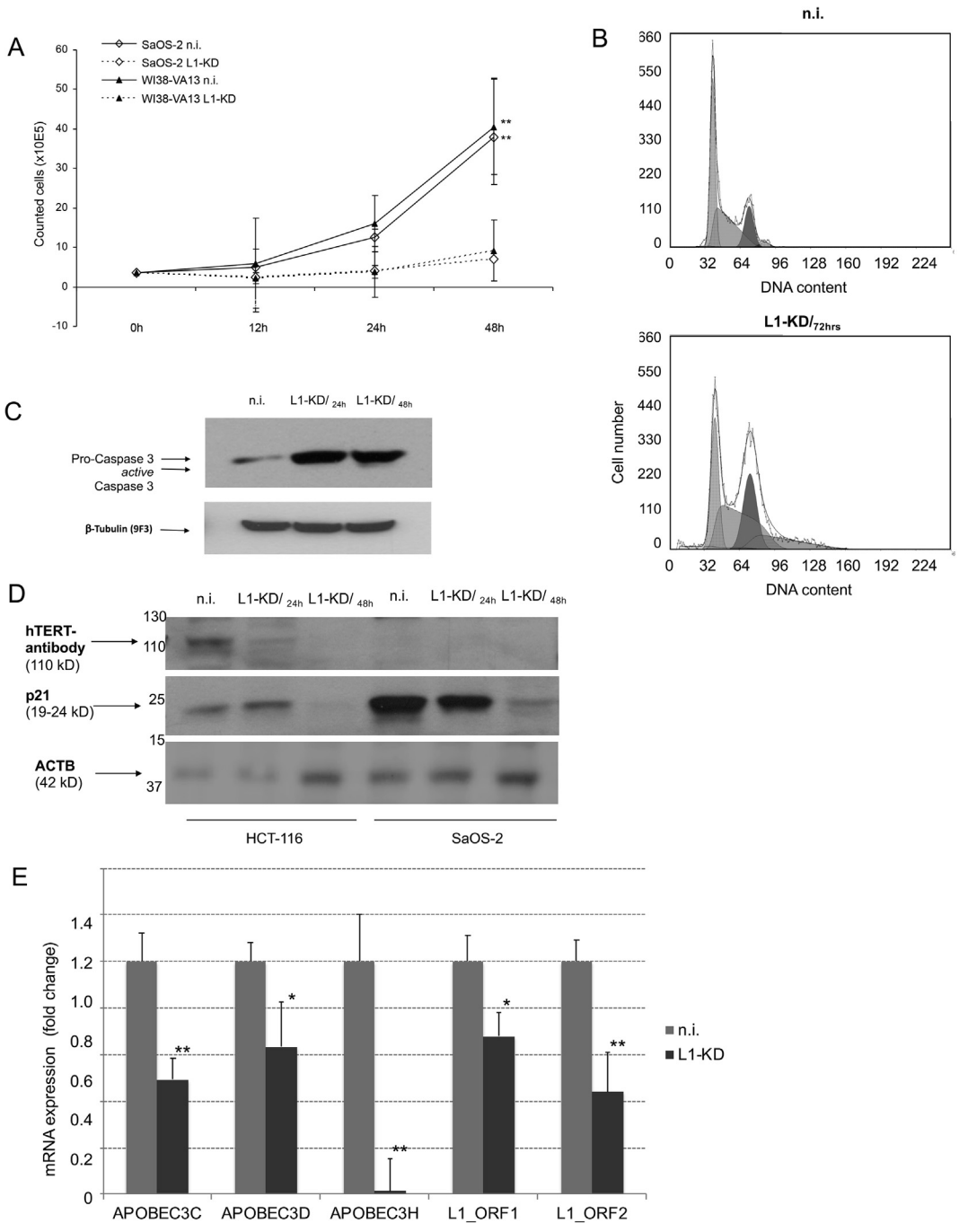

Fig. 3. L1-RNP is associated with cell growth, cell senescence and metabolism. A, L1-KD shows reduced cell growth in ALT cell lines (SaOS-2 and WI38-VA13/2RA) compared to scrambled siRNA-KD. Cell counts and timeline as indicated. n = 3. B, Representative images of DNA content during cell cycle measured by PI staining and flow cytometry analysis. G0/G1-, S- and G2/M-phase as indicated. C and D, L1-KD leads to cell death by activation of caspase 3 (C) and *p*21 inhibition (D). Assays were done in ALT$^+$ cells 24 h and 48 h after L1-KD as indicated by western blot analysis. Internal standards and protein marker size are indicated. E, APOBECs mRNA expression were reduced after L1-KD. n = 2; error bars are s.e.m. *) $p < 0.05$, **) $p < 0.01$.

L1-RNP expression supports molecular characteristics of ALT phenotype

An important structural part of telomeres in ALT$^+$ cells is TERRA, a telomeric RNA transcribed from sub-telomeric regions [24]. The vast majority of TERRA sequences lack poly-adenylation (poly(A)) processing and remain in the nucleus supporting their function in telomere regulation and stabilization. About 8% of TERRA is polyadenylated [29,70]. However, most of the polyadenylated TERRA is still retained in the nucleus, and only a negligible quantity of TERRA is usually detected in the cytoplasm [29].

In order to investigate an association of L1-RNP and TERRA we visualized TERRA by FISH analysis in ALT$^+$ cell lines treated by L1-KD. In non-treated and scrambled-treated cells all TERRA signals are confined to

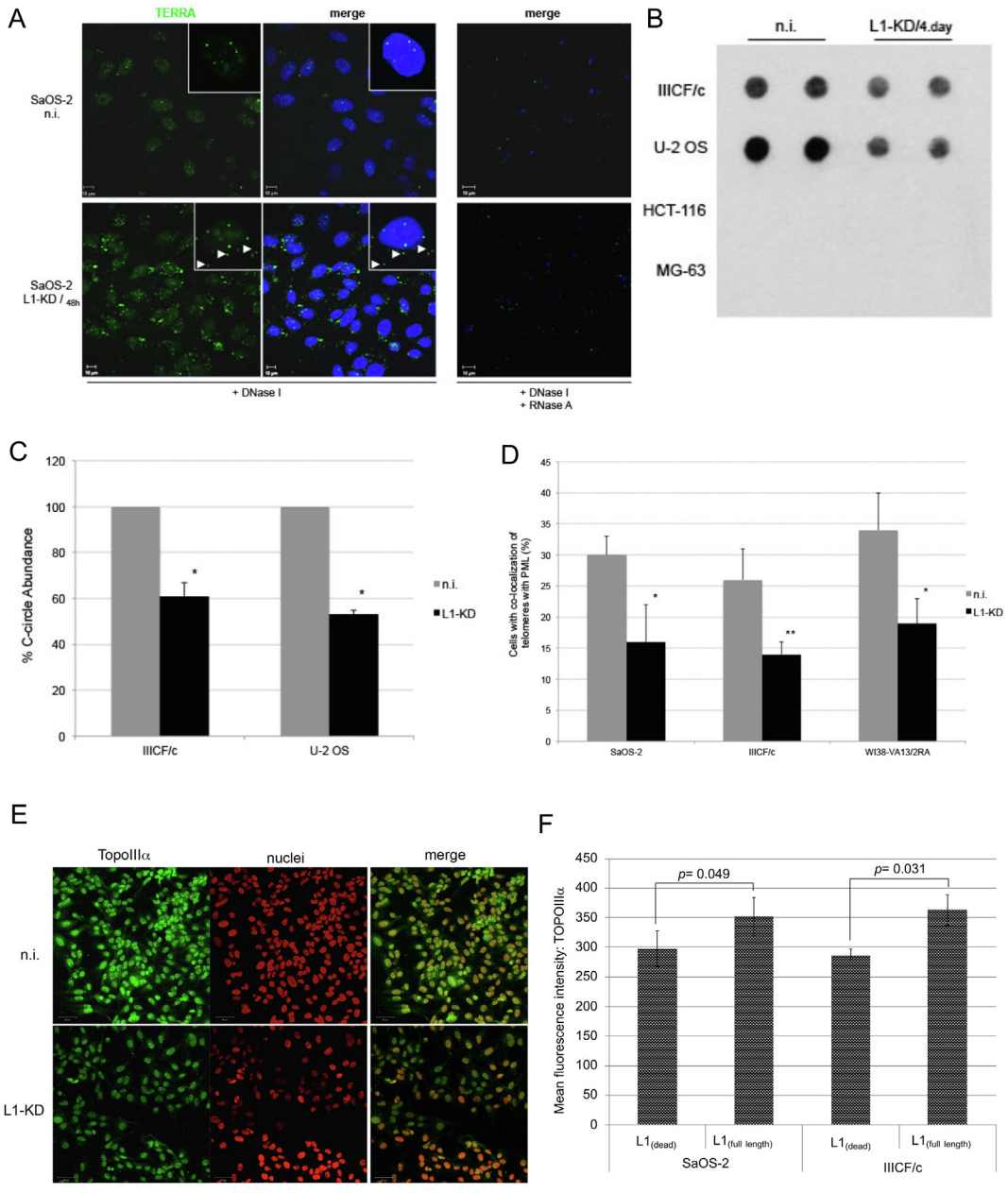

Fig. 4. L1-KD is associated with a loss of telomere stability. A, L1-KD promotes extra-nuclear TERRA foci (arrows) in SaOS-2 cells. As control, DNaseI and RNaseA treated cells given on the right. TERRA, green; DNA, blue. B, C, L1-KD reduces c-circle activity in U-2 OS and IIICF/c cells as determined by CC-assay, compared to non-interfering siRNA treatment (n.i.). Percentage of c-circle abundance is given as diagram (B). n = 2; error bars are s.d. *) $p < 0.05$. Dot blots (C) represents amplified telomeric $(CCCTAA)_n$ circles. Cell lines and treatment as indicated. TA^+ cell lines HCT-116 and MG-63 were used as negative control. D, Statistical analysis of reduced PML bodies co-localized with telomeres. *) $p < 0.05$; **) $p < 0.01$n = 3; mean þ s.d. E, TopoIIIα was regulated by L1-KD in different ALT^+ cell lines. TopoIIIα-protein levels during L1-KD with L1-RNP-siRNA were measured by ICC staining. Representative images are shown. green, TopoIIIα-protein, red, DNA staining. Scale bar, 20 μm. F, LINE-1 overexpression leads to increased TopoIIIα-protein levels done by L1-mRNA plasmid transfection (L1-full length) compared to control plasmid (L1-dead) in ALT^+ cells (as indicated). Statistical analysis of immunofluorescence analysis by mean fluorescence intensity of TopoIIIα antibody staining is given. *p*-values are given on the top. Cell lines are given at the bottom. n = 3; mean þ s.d.

the nucleus in this assay. In contrast, in L1-KD treated cells TERRA was also found in the cytoplasm at substantial quantities (Fig. 4A and Supplementary Fig. 7).

TERRA/PML co-localization is important for successful stabilization of telomeres [71]. During L1-KD, we observed a reduced abundance of TERRA/PML co-localisation (Supplementary Fig. 8). These data support the idea of poly(A)$^+$ TERRA binding affinity to the L1-RNP-RNA binding site, which were dispersed by L1-KD.

C-circles and APB formation are one of the most relevant hallmarks of ALT activity. C-circles were significantly decreased in L1-KD treated ALT^+ cells as compared to control (Fig. 4, *B and C*). TA^+ tumor cell lines were used as negative control for the c-circle assay. Similarly, APB bodies

were also significantly reduced in L1-KD treated ALT$^+$ tumor cells as compared to non-interfering-siRNA treated controls, concordant to the previously described reduction of TERRA/PML co-localization (Fig. 4D and Supplementary Fig. 9).

Another essential feature of the ALT phenotype is the expression of topoisomerase IIIα (TopoIIIα). KD of TopoIIIα (TopoIIIα-KD) leads to G2/M arrest and a reduced level of cell viability in ALT$^+$ cells [32]. We performed comparative experiments with L1-KD and TopoIIIα-KD (Supplementary Fig. 10). Furthermore, we tested the effect of L1-RNP-siRNAs on TopoIIIα protein expression using siRNA. Interestingly, L1-RNP-siRNA also resulted in reductions of TopoIIIα protein levels (Fig. 4E). The level of TopoIIIα mRNA and protein reduction correlated with the efficacy of L1-RNP-specific siRNA (Supplementary Fig. 11). In contrast, L1-overexpression by L1-full length sequence expression plasmid transfection (L1-full length) in ALT$^+$ cells did increase TopoIIIα protein expression (Fig. 4F), while knockdown of TopoIIIα did not alter the L1-RNP-expression (data not shown). Collectively, these results indicate, that L1-RNP seems to regulate TMM upstream of TopoIIIα expression.

L1-RNP proteins bind to telomeric ends and to TERRA

We next analyzed a potential molecular interaction between L1-RNP and telomeric DNA. ICC and ChIP analysis revealed a binding of L1-RNP to telomeric DNA in ALT$^+$ (Fig. 5, *A and B*). TRF-2 binding to telomeric sequences was used as a positive control. Using purified L1-RNP indicated a binding of L1-RNP-ORF1 to the telomeric C-strand but not to the telomeric G-strand by using the band shift assay (Fig. 5C).

Since ALT$^+$ cells are also known to express high levels of TERRA [24] and since the *ORF1*-encoded protein of the L1-RNP element is an RNA-binding protein [42], we assumed a possible binding of L1-RNP to TERRA-specific sequences. RNA-immunoprecipitation (RNA-IP) performed with ALT cell extracts confirmed this binding but not to the complementary sequences (Fig. 5D). The known binding of TRF2 and TRF1 to TERRA [27] was used as a positive control. We did not observe a binding of L1-RNP to TRF2 or other Shelterin proteins further suggesting direct binding of L1-RNP to TERRA (Supplementary Fig. 12).

The polyadenylation of RNA sequences is essential for the RNA binding to the L1-RNP-ORF1 protein [72]. As we detected elevated cytoplasmic TERRA in L1-KD ALT$^+$ cells we hypothesized, that L1-RNP could preferentially bind to poly(A)-TERRA retaining this TERRA in the nucleus. We therefore performed a TERRA/L1-RNP-specific binding assay using purified L1-RNP proteins (L1-ORF1 and L1-RT) and synthetic TERRA constructs. The results indicated a binding of L1-ORF1 protein to poly(A)$^+$TERRA but not to poly(A)$^-$TERRA (Fig. 5E).

Reverse transcriptase inhibition leads to L1-RNP upregulation

It is known that L1-RNP has the ability to switch RNA templates [42]. Since we demonstrated binding of L1-RNP to TERRA, we tested whether L1-RNP synthesizes telomeric TTAGGG-DNA sequences using TERRA as a template. Therefore, we performed an L1-RNP-specific *in-vitro*-RT reaction as described previously [60]. Dot blot hybridisation indicated that purified L1-RNP protein could generate a product complementary to TERRA in ALT$^+$ cell lines but not in TA$^+$ cell lines (Fig. 6A). L1-KD abrogated the generation of this telomere-specific product further suggesting an L1-RNP-specific effect (Supplementary Fig. 13).

To analyze the importance of L1-RNP-RT activity for telomeric stabilization, we investigated the effect of reverse transcriptase inhibitors (RTI) on U2-OS ALT$^+$ cell line. We treated ALT$^+$ cells with either azidothymidine (AZT), didanosine (ddI) or with the combination of both drugs for 5 days. Those drugs have been described to inhibit L1-RNP-specific RT activity [46]. The combination of RTIs led to a significant increase in the number of TIFs but also augmented the number of overall DNA strand breaks (Fig. 6B and Supplementary Fig. 14). The increase in DNA damage was correlated with a significant increase of L1-RNP protein and L1-RNP mRNA expression, as determined by ICC, WB and RT-qPCR (Fig. 6, *C and D* and Supplementary Fig. 15). Correspondingly, inhibition of the RT activity did not lead to a significant inhibition of cell growth (Supplementary Fig. 16). However, in concordance with our hypothesis that L1-RNP regulates ALT, we observed an increase of c-circle activity in RTI treated cells, compared to mock-treated ALT$^+$ cells (Fig. 6E).

To confirm ALT activation after L1 induction, we analyzed L1 overexpression (L1-OE) in ALT$^+$ cells done by plasmid transfection with full length L1-sequences (L1-full length) compared to inactive control plasmid transfection (L1-dead) (Supplementary Fig. 17). We observed a positive modulation of ALT characteristics, determined by an increase of TERRA expression and c-circle production (Fig. 6F, and Supplementary Fig. 18). In TA$^+$ cell lines L1-RNPs plays a clear role in both, KLF4 and cMyc gene regulation. In contrast, in ALT cells we only observed a decrease of KLF4 expression after L1-KD, but there were no detectable changes in upregulation of KLF4 during L1-OE (Supplementary Fig. 19). cMyc levels were only marginally detected in our cell lines and showed no difference in protein or mRNA expression during up- or downregulation of L1-RNPs (data not shown).

Discussion

Our present study highlights a contribution of L1-RNP to TMM in ALT$^+$ cancer cells. We demonstrate that L1-RNP expression is more pronounced in ALT$^+$ compared to TA$^+$ in human GBM. High levels of L1-RNP expression and correlating hypomethylation of L1-RNP genomic copies have also been described in aggressive and highly malignant tumors with fatal outcome (e.g. GBM, rhabdomyosarcoma or other soft tissue tumors), which frequently uses ALT as TMM [73–75]. The increased levels of L1-RNP in ALT$^+$/TA$^-$ GBM specimens can be explained by the decreased expression of ATRX. ATRX/H3.3 chaperone protein complex is required for silencing of endogenous retroviral elements [76].

To further investigate a possible correlation of L1-RNP and ALT, we used well-established ALT$^+$ tumor cell lines. L1-RNP expression in ALT$^+$ cell lines supported all characteristic features of ALT such as c-circles, PML bodies, nuclear localisation of TERRA and TopoIIIα. Thus, down-regulation of L1-RNP led to a decrease in telomere integrity as indicated by an increased number of TIFs explaining the concomitant occurrence of anaphase bridges. Shay et al. proposed that ALT was not supported by one single mechanism, but by multiple different regulations [16]. Thus, L1-RNP might be one of those regulatory factors.

Possibly the most relevant feature of L1-RNP for TMM regulation of ALT is its binding affinity to poly(A)-TERRA. Porro et al. has demonstrated that despite its poly(A)-tail the majority of poly(A)$^+$TERRA was found in the nucleus [29]. With respect to our results of RNA-*Q-FISH* and RNA-EMSA, we suggest that the L1-RNP-binding of TERRA may be essential for its nuclear localisation. This is relevant for ALT as TERRA appears to be a key-factor for homologous recombination (HR) in ALT$^+$ cells as it facilitates binding of replication protein A [29]. Moreover, the number of RNA-DNA hybrids formed by TERRA and telomeric DNA were found to be critical for HR and subsequently for TMM in ALT [20]. Based on the decrease in HR observed after L1-KD, we conclude that this is due to the fact that L1-RNP links poly(A) TERRA to telomeric sites. TERRA also appears to serve as a scaffold for telomere stability [71]. In this context, Porro et al. described an involvement of TERRA to protect open telomeric 3′ G strands [29]. We now suggest that L1-RNP indirectly supports the stability of telomeric ends by ensuring sufficient levels of TERRA at the telomeric sites. Thus, increased L1-KD associated TIFs

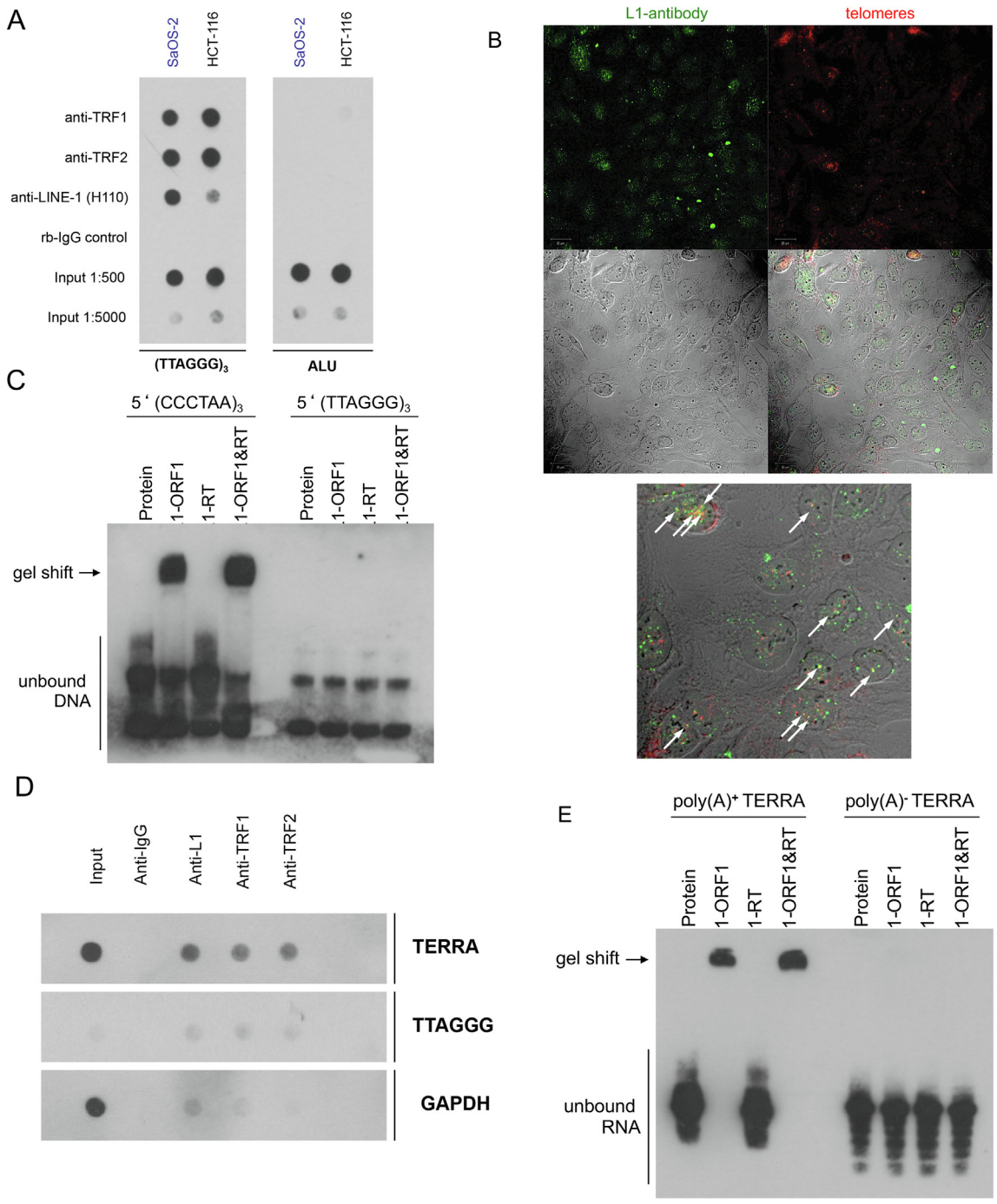

Fig. 5. Association of L1-RNP to telomeric ends and TERRA. A, Binding of L1-RNP to telomeric DNA in cell lysates. Representative telomeric ChIP experiment indicates binding of L1-RNP to telomeric repeats preferred in ALT^{+} (SaOS-2), compared to TA^{+}(HCT-116) cell lysates. $(TTAGGG)_3$ sequence for telomeric binding, ALU sequence as negative binding control. TRF1 and TRF2 were used as positive controls; rabbit-IgG antibody was used as negative control. Each ChIP was done for at least three independent experiments. Input dilutions are DNA extract from non-purified protein samples. B, Representative images of *Q-FISH* assay, performed on ALT + cell line IIICF/c, indicates L1-RNP (green, L1-antibody) binding to telomeres (red, FITC-TTAGGG-PNA-probe). Cell nuclei are figured by reflected light microscopy. Enlarged image shows co-localization (white arrows). C, Binding of purified L1-RNP- to telomeric DNA. DNA-EMSA, performed with purified L1-RNP-ORF1- and L1-RNP-RT-proteins, indicating binding of L1-RNP-ORF1 to the telomeric C-strand (5′-CCCTAA), but not G-strand (5′-TTAGGG). Each DNA-EMSA was done for at least three times. D, RNA immunoprecipitation using L1-RNP antibody demonstrating the binding of L1-RNP to TERRA sequence (UUAGGG) but not to complementary RNA sequence (CCCUAA), performed with SaOS-2 cell extracts. GAPDH was used as control. Specific probes are given on the right. n = 3. E, RNA-EMSA assay performed with purified L1-RNPs (L1-ORF1 and L1-RT) indicating binding of L1-ORF1 to the poly(A)$^{+}$ TERRA sequence, but not poly(A)$^{-}$ TERRA sequence. Each EMSA was done for at least three times.

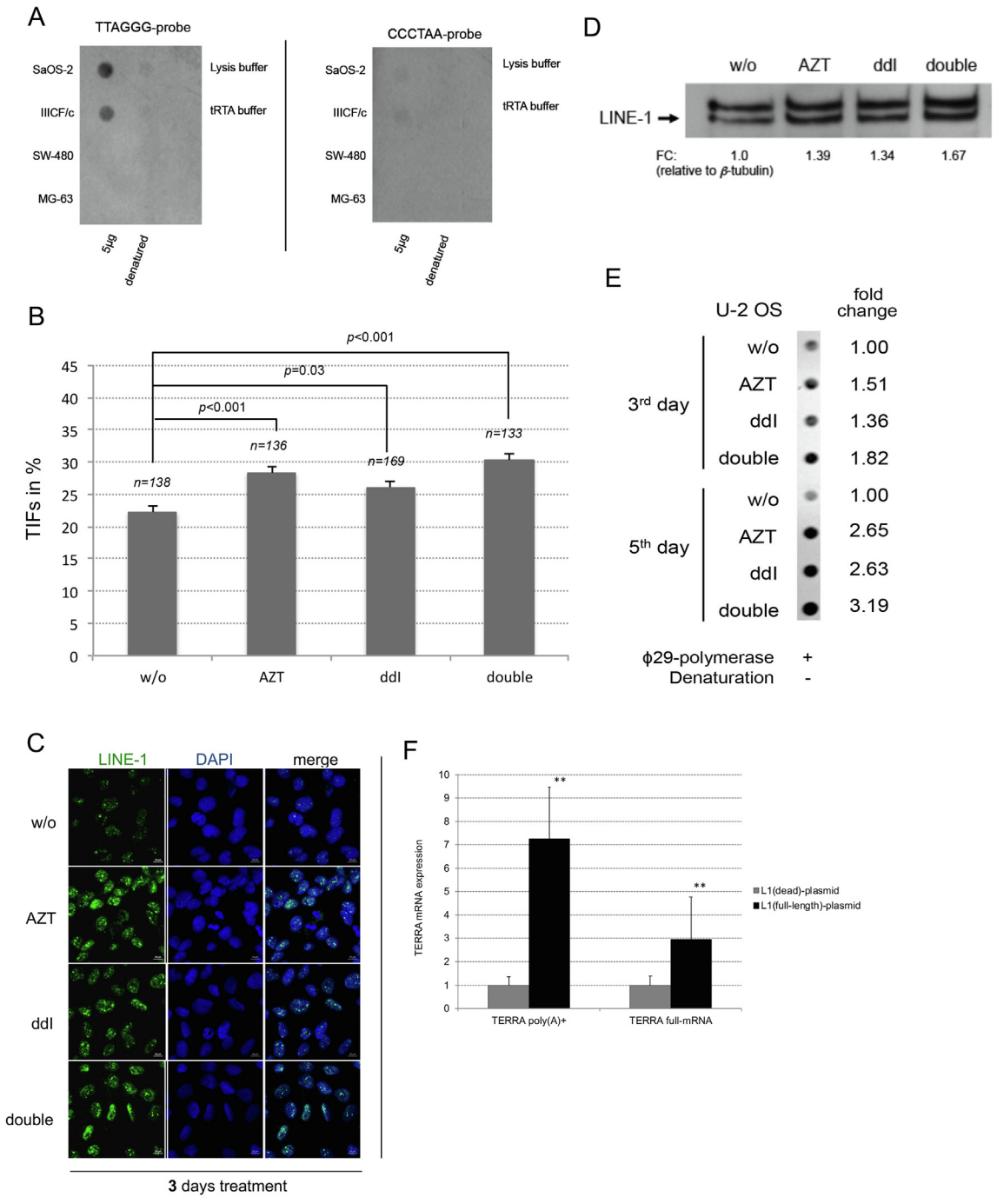

Fig. 6. L1-RNP-RT activity and RT-inhibition of ALT$^+$ cell lines. A, TERRA-specific RT activity in ALT cell lysates (5 µg): Telomeric sequences complementary to TERRA are produced *in-vitro* in ALT$^+$-(SaOS-2 and IIICF/c) but not in TA$^+$-lysates (SW-480 and MG-63). RT-assay followed by dot blot hybridization showing strand specificity. Products, which are produced with TERRA as template, are on the left blot (TTAGGG-probe), for complementary sequence on the right blot (CCCTAA-probe). Heated samples (denatured proteins) were used to determine background signals. Cell lines as indicated on the left. n = 3. B, RTI treatment significantly increases TIFs in ALT$^+$ cell line. n, number of counted nuclei of two independent experiments. *p*-value is indicated on the top. mean þ s.d. Assay was done for at least three times. C, representative image of L1-RNP level measurements done by ICC (C) and western blot (D) after 3 days of different and combined RTI treatment. ICC staining: L1-RNP, green; DNA staining, DAPI blue. Western blot: L1-RNP antibody signal was found between 140–150 kDa. Fold change (FC) relative to β-tubulin is given at the bottom. E, Representative image of c-circle assay show an increase of c-circle activity during L1-RNP-upregulation in U-2 OS ALT$^+$cell line, after 3 and 5 days after treatment as indicated. w/o, untreated cells; AZT, azidothymidine; ddi, didanosine; double, AZT and ddI. F, LINE-1 overexpression leads to increased TERRA levels done by L1-mRNA plasmid transfection (black bars, L1-full length) compared to control plasmids (gray bars, L1-dead) in ALT$^+$ cells (as indicated) three days after treatment start. Statistical analysis of TERRA expression done by RT-qPCR is given. Specific TERRA primers are given at the bottom. n = 3; mean þ s.d. **) $p < 0.01$.

can be explained by the lack of nuclear TERRA. L1-KD associated telomeric dysfunction can further be due to a reduction of APBs, which are a prerequisite for BIR [23], but might also rely on the downregulation of TopoIIIα preventing efficient formation of the BTR-complex [31] and subsequent reduced generation of novel telomere sequences.

In contrast to TA$^+$ cells, we have not observed a L1-KD induced decrease of TL in ALT + cells. The most likely reason is the fact that telomeres are found to be 4 to 7-fold longer in ALT$^+$- as compared to TA$^+$ tumor cells [12]. An absence of significant telomere shortening in ALT$^+$ cells could be explained by the short duration of siRNA treatment, within 5 population doublings.

The RT activity of L1-RNP has the ability to switch the RNA template [42] with an high avidity for TERRA. Using cell extracts we demonstrated that the reverse transcriptase of L1-RNPs is able to generate telomere specific sequences. Thus, L1-RNP could ensure TMM in ALT$^+$ cells not only by a scaffold function to keep TERRA at the telomeric ends but also by the generation of novel telomeric sequences. However, in contrast to LINE-1-specific siRNA, RTI treatment with DDI and AZT did not reveal a decrease in tumor cell growth but an increase in expression of L1-RNPs and c-circles. This therapeutically negative finding suggests two possible interpretations: i) The RT activity of L1-RNPs is not relevant for TMM in ALT$^+$ cells. L1-RNP -upregulation is part of the response to genomic DNA damage and independent of telomere dysfunction. ii) Alternatively, RTI-induced increase in L1-RNP might be a feedback loop of dysfunctional L1-RNP-RT. Higher levels of L1-RNP-RT could neutralize RTIs used in low doses. However, the correlation of RTI-induced L1-RNP upregulation with the increase in c-circles still strongly support a role of L1-RNPs in ALT regulation.

Retrotransposons are regarded as retroviral elements [49]. A retrotranscription of TERRA by L1-RNP might lead to c-circles observed in ALT. Extra-chromosomal circular DNA such as c-circles have most recently shown to induce type I INF via the STING/cGAS pathway, which are downregulated in ALT$^+$ cells to ensure cellular survival [77]. An association of c-circles with retroviruses-related retrotransposons, which are regarded foreign due to their viral origin, can now explain the fact that c-circles induce an immune response.

L1-KD reduces growth of TA$^+$ cancer cells [51–53] due to reduced transcriptional induction of hTERT and c-Myc by L1-RNP elements. TA$^+$ cells have low levels of TERRA because hTERT inhibits TERRA [78]. Moreover, ALT$^+$ cell lines have reduced oncogene expression of cMyc and KLF-4 comparable to the TA$^+$ cell lines [79]. Apparently, the mechanism how L1-RNP supports TMM in TA$^+$ versus ALT$^+$ cell lines is differently regulated but would suggest that L1-RNP has a general co-factor role to support telomere integrity. Most recently, L1-RNP activation has been shown to regulate global chromatin accessibility in early mouse embryos [80]. L1-RNP induced global chromatin regulation also correlates with its impact on senescence and the activation of type I IFN leading to inflammaging [81]. With respect to senescence we also observed a downregulation of p21 by inhibition of LINE-1 in an ALT cell line apart of its concomitant regulation of Shelterins and TopoIIIα. Given the role of L1-RNP in TA$^+$ cells cancer-associated reactivation of L1-RNP regulating global chromatin accessibility appears to promote transcription of multiple genes involved in proliferation, cell survival and telomere regulation independent of the specific TMM.

Conclusion

In this study, we describe a new essential function of L1-RNP for TMM in ALT$^+$ cells aside from its known function to support genetic diversity. We propose that an L1-RNP targeting therapy unrelated to its RT activity will not only be effective in TA$^+$ but also ALT$^+$-tumor cells. Targeting L1-RNP protein in cancer therapy, which might be possible via epigenetic modulation inducing H3K9me3 [76,82] would ideally complement current telomerase inhibitors to prevent escape phenomena [16].

Funding

Supported in part by grants from the Medical-Scientific Fund of the Mayor of Vienna (Project- No. 15155 to TA and Project Nr. 15071 to MB).

Acknowledgment

We want to thank Jef D. Boeke for plasmids expressing L1-RNP proteins and to Roger Reddel for providing cell lines.

Competing interests

The authors declare that they have no competing interests related to the present work. MB received consultant fees from Bristol Myers Squibb, Takeda and Dr. Falk Pharma. MB is a founding member of Vacthera GesmbH, Vienna.

Appendix A. Supplementary data

Supplementary data to this article can be found online at https://doi.org/10.1016/j.neo.2019.11.002.

References

1. Blackburn EH. Telomeres. *Trends Biochem Sci* 1991;**16**:378–81.
2. Karlseder J, Smogorzewska A, de Lange T. Senescence induced by altered telomere state, not telomere loss. *Science* 2002;**295**:2446–9.
3. de Lange T. Shelterin: the protein complex that shapes and safeguards human telomeres. *Genes Dev* 2005;**19**:2100–10.
4. Fumagalli M, Rossiello F, Clerici M, Barozzi S, Cittaro D, Kaplunov JM, Bucci M, Dobreva M, Matti V, Beausejour CM, et al. Telomeric DNA damage is irreparable and causes persistent DNA-damage-response activation. *Nat Cell Biol* 2012;**14**:355–65.
5. Griffith JD, Comeau L, Rosenfield S, Stansel RM, Bianchi A, Moss H, de Lange T. Mammalian telomeres end in a large duplex loop. *Cell* 1999;**97**:503–14.
6. Martinez P, Blasco MA. Telomeric and extra-telomeric roles for telomerase and the telomere-binding proteins. *Nat Rev Cancer* 2011;**11**:161–76.
7. Choi KH, Farrell AS, Lakamp AS, Ouellette MM. Characterization of the DNA binding specificity of Shelterin complexes. *Nucleic Acids Res* 2011;**39**:9206–23.
8. Harley CB, Futcher AB, Greider CW. Telomeres shorten during ageing of human fibroblasts. *Nature* 1990;**345**:458–60.
9. Greider CW, Blackburn EH. The telomere terminal transferase of Tetrahymena is a ribonucleoprotein enzyme with two kinds of primer specificity. *Cell* 1987;**51**:887–98.
10. Blackburn EH, Greider CW, Henderson E, Lee MS, Shampay J, Shippen-Lentz D. Recognition and elongation of telomeres by telomerase. *Genome* 1989;**31**:553–60.
11. Shippen-Lentz D, Blackburn EH. Functional evidence for an RNA template in telomerase. *Science* 1990;**247**:546–52.
12. Henson JD, Neumann AA, Yeager TR, Reddel RR. Alternative lengthening of telomeres in mammalian cells. *Oncogene* 2002;**21**:598–610.
13. Cesare AJ, Reddel RR. Alternative lengthening of telomeres: models, mechanisms and implications. *Nat Rev Genet* 2010;**11**:319–30.
14. Lee CY, Horn HF, Stewart CL, Burke B, Bolcun-Filas E, Schimenti JC, Dresser ME, Pezza RJ. Mechanism and regulation of rapid telomere prophase movements in mouse meiotic chromosomes. *Cell Rep* 2015;**11**:551–63.
15. Deng Z, Wang Z, Xiang C, Molczan A, Baubet V, Conejo-Garcia J, Xu X, Lieberman PM, Dahmane N. Formation of telomeric repeat-containing RNA

(TERRA) foci in highly proliferating mouse cerebellar neuronal progenitors and medulloblastoma. *J Cell Sci* 2012;**125**:4383–94.
16. Shay JW, Reddel RR, Wright WE. Cancer. Cancer and telomeres–an ALTernative to telomerase. *Science* 2012;**336**:1388–90.
17. Chudasama P, Mughal SS, Sanders MA, Hubschmann D, Chung I, Deeg KI, Wong SH, Rabe S, Hlevnjak M, Zapatka M, et al. Integrative genomic and transcriptomic analysis of leiomyosarcoma. *Nat Commun* 2018;**9**:144.
18. Napier CE, Huschtscha LI, Harvey A, Bower K, Noble JR, Hendrickson EA, Reddel RR. ATRX represses alternative lengthening of telomeres. *Oncotarget* 2015;**6**:16543–58.
19. Li F, Deng Z, Zhang L, Wu C, Jin Y, Hwang I, Vladimirova O, Xu L, Yang L, Lu B, et al. ATRX loss induces telomere dysfunction and necessitates induction of alternative lengthening of telomeres during human cell immortalization. *EMBO J* 2019;**38** e96659.
20. Arora R, Lee Y, Wischnewski H, Brun CM, Schwarz T, Azzalin CM (2014). RNaseH1 regulates TERRA-telomeric DNA hybrids and telomere maintenance in ALT tumour cells Nat Commun 5, 5220.
21. Henson JD, Cao Y, Huschtscha LI, Chang AC, Au AY, Pickett HA, Reddel RR. DNA C-circles are specific and quantifiable markers of alternative-lengthening-of-telomeres activity. *Nat Biotechnol* 2009;**27**:1181–5.
22. Chung I, Osterwald S, Deeg KI, Rippe K. PML body meets telomere: the beginning of an ALTernate ending? *Nucleus* 2012;**3**:263–75.
23. Zhang JM, Yadav T, Ouyang J, Lan L, Zou L. Alternative lengthening of telomeres through two distinct break-induced replication pathways. *Cell Rep* 2019;**26**(955–968) e953.
24. Luke B, Lingner J. TERRA: telomeric repeat-containing RNA. *EMBO J* 2009;**28**:2503–10.
25. Yu TY, Kao YW, Lin JJ. Telomeric transcripts stimulate telomere recombination to suppress senescence in cells lacking telomerase. *Proc Natl Acad Sci U S A* 2014;**111**:3377–82.
26. Schoeftner S, Blasco MA. A 'higher order' of telomere regulation: telomere heterochromatin and telomeric RNAs. *EMBO J* 2009;**28**:2323–36.
27. Deng Z, Norseen J, Wiedmer A, Riethman H, Lieberman PM. TERRA RNA binding to TRF2 facilitates heterochromatin formation and ORC recruitment at telomeres. *Mol Cell* 2009;**35**:403–13.
28. Azzalin CM, Reichenbach P, Khoriauli L, Giulotto E, Lingner J. Telomeric repeat containing RNA and RNA surveillance factors at mammalian chromosome ends. *Science* 2007;**318**:798–801.
29. Porro A, Feuerhahn S, Lingner J. TERRA-reinforced association of LSD1 with MRE11 promotes processing of uncapped telomeres. *Cell Rep* 2014;**6**:765–76
30. Sobinoff AP, Pickett HA. Alternative lengthening of telomeres: DNA repair pathways converge. *Trends Genet* 2017;**33**:921–32.
31. Sobinoff AP, Allen JA, Neumann AA, Yang SF, Walsh ME, Henson JD, Reddel RR, Pickett HA. BLM and SLX4 play opposing roles in recombination-dependent replication at human telomeres. *EMBO J* 2017;**36**:2907–19.
32. Temime-Smaali N, Guittat L, Wenner T, Bayart E, Douarre C, Gomez D, Giraud-Panis MJ, Londono-Vallejo A, Gilson E, Amor-Gueret M, et al. Topoisomerase IIIalpha is required for normal proliferation and telomere stability in alternative lengthening of telomeres. *EMBO J* 2008;**27**:1513–24.
33. Pan X, Drosopoulos WC, Sethi L, Madireddy A, Schildkraut CL, Zhang D. FANCM, BRCA1, and BLM cooperatively resolve the replication stress at the ALT telomeres. *Proc Natl Acad Sci U S A* 2017;**114**:E5940–9.
34. Lu R, O'Rourke JJ, Sobinoff AP, Allen JAM, Nelson CB, Tomlinson CG, Lee RR, Reddel RR, Deans AJ, Pickett HA. The FANCM-BLM-TOP3A-RMI complex suppresses alternative lengthening of telomeres. *(ALT) Nat Commun* 2019;**10**:2252.
35. O'Rourke JJ, Bythell-Douglas R, Dunn EA, Deans AJ (2019). ALT control, delete: FANCM as an anti-cancer target in Alternative Lengthening of Telomeres. Nucleus.
36. Shay JWRR, Wright WE. Cancer. Cancer and telomeres–an ALTernative to telomerase. *Science* 2012;**336**:1388–90.
37. Verma P, Dilley RL, Zhang T, Gyparaki MT, Li Y, Greenberg RA. RAD52 and SLX4 act nonepistatically to ensure telomere stability during alternative telomere lengthening. *Genes Dev* 2019;**33**:221–35.
38. Sugarman ET, Zhang G, Shay JW. perspective: an update on telomere targeting in cancer. *Mol Carcinog* 2019;**58**:1581–8.
39. Brouha B, Schustak J, Badge RM, Lutz-Prigge S, Farley AH, Moran JV, Kazazian Jr HH. Hot L1s account for the bulk of retrotransposition in the human population. *Proc Natl Acad Sci U S A* 2003;**100**:5280–5.
40. Morrish TA, Gilbert N, Myers JS, Vincent BJ, Stamato TD, Taccioli GE, Batzer MA, Moran JV. DNA repair mediated by endonuclease-independent LINE-1 retrotransposition. *Nat Genet* 2002;**31**:159–65.
41. Luan DD, Korman MH, Jakubczak JL, Eickbush TH. Reverse transcription of R2Bm RNA is primed by a nick at the chromosomal target site: a mechanism for non-LTR retrotransposition. *Cell* 1993;**72**:595–605.
42. Kolosha VO, Martin SL (2003). High-affinity, non-sequence-specific RNA binding by the open reading frame 1 (ORF1) protein from long interspersed nuclear element 1 (LINE-1) J Biol Chem 278, 8112–8117.
43. Feng Q, Moran JV, Kazazian Jr HH, Boeke JD. Human L1 retrotransposon encodes a conserved endonuclease required for retrotransposition. *Cell* 1996;**87**:905–16.
44. An W, Dai L, Niewiadomska AM, Yetil A, O'Donnell KA, Han JS, Boeke JD. Characterization of a synthetic human LINE-1 retrotransposon ORFeus-Hs. *Mob DNA* 2011;**2**:2.
45. Garcia-Perez JL, Marchetto MC, Muotri AR, Coufal NG, Gage FH, O'Shea JV, Moran JV. LINE-1 retrotransposition in human embryonic stem cells. *Hum Mol Genet* 2007;**16**:1569–77.
46. De Luca C, Guadagni F, Sinibaldi-Vallebona P, Sentinelli S, Gallucci M, Hoffmann A, Schumann GG, Spadafora C, Sciamanna I (2016). Enhanced expression of LINE-1-encoded ORF2 protein in early stages of colon and prostate transformation Oncotarget 7, 4048–4061.
47. Scott AF, Schmeckpeper BJ, Abdelrazik M, Comey CT, O'Hara B, Rossiter JP, Cooley T, Heath P, Smith KD, Margolet L (1987). Origin of the human L1 elements: proposed progenitor genes deduced from a consensus DNA sequence Genomics 1, 113–125.
48. Kano H, Godoy I, Courtney C, Vetter MR, Gerton GL, Ostertag EM, Kazazian Jr HH. L1 retrotransposition occurs mainly in embryogenesis and creates somatic mosaicism. *Genes Dev* 2009;**23**:1303–12.
49. Beck CR, Collier P, Macfarlane C, Malig M, Kidd JM, Eichler EE, Badge RM, Moran JV. LINE-1 retrotransposition activity in human genomes. *Cell* 2010;**141**:1159–70.
50. Vitullo P, Sciamanna I, Baiocchi M, Sinibaldi-Vallebona P, Spadafora C (2012). LINE-1 retrotransposon copies are amplified during murine early embryo development Mol Reprod Dev 79, 118–127.
51. Aschacher T, Wolf B, Enzmann F, Kienzl P, Messner B, Sampl S, Svoboda M, Mechtcheriakova D, Holzmann K, Bergmann M. LINE-1 induces hTERT and ensures telomere maintenance in tumour cell lines. *Oncogene* 2016;**35**:94–104
52. Sciamanna I, Landriscina M, Pittoggi C, Quirino M, Mearelli C, Beraldi R, Mattei E, Serafino A, Cassano A, Sinibaldi-Vallebona P, et al. Inhibition of endogenous reverse transcriptase antagonizes human tumor growth. *Oncogene* 2005;**24**:3923–31.
53. Oricchio E, Sciamanna I, Beraldi R, Tolstonog GV, Schumann GG, Spadafora C (2007). Distinct roles for LINE-1 and HERV-K retroelements in cell proliferation, differentiation and tumor progression Oncogene 26, 4226–4233.
54. Sampl S, Pramhas S, Stern C, Preusser M, Marosi C, Holzmann K. Expression of telomeres in astrocytoma WHO grade 2 to 4: TERRA level correlates with telomere length, telomerase activity, and advanced clinical grade. *Transl Oncol* 2012;**5**:56–65.
55. Lotsch D, Ghanim B, Laaber M, Wurm G, Weis S, Lenz S, Webersinke G, Pichler J, Berger W, Spiegl-Kreinecker S. Prognostic significance of telomerase-associated parameters in glioblastoma: effect of patient age. *Neuro Oncol* 2013;**15**:423–32.
56. Lamprecht MR, Sabatini DM, Carpenter AE. Cell Profiler: free, versatile software for automated biological image analysis. *Biotechniques* 2007;**42**:71–5.
57. Aschacher T, Sampl S, Kaser L, Bernhard D, Spittler A, Holzmann K, Bergmann M. The combined use of known antiviral reverse transcriptase inhibitors AZT and DDI induce anticancer effects at low concentrations. *Neoplasia* 2012;**14**:44–53.
58. Henson JD, Lau LM, Koch S, Martin La Rotta N, Dagg RA, Reddel RR (2017). The C-Circle Assay for alternative-lengthening-of-telomeres activity Methods 114, 74–84.
59. Hellman LM, Fried MG. Electrophoretic mobility shift assay (EMSA) for detecting protein-nucleic acid interactions. *Nat Protoc* 2007;**2**:1849–61.
60. Dai L, Huang Q, Boeke JD. Effect of reverse transcriptase inhibitors on LINE-1 and Ty1 reverse transcriptase activities and on LINE-1 retrotransposition. *BMC Biochem* 2011;**12**:18.
61. Cost GJ, Feng Q, Jacquier A, Boeke JD. Human L1 element target-primed reverse transcription in vitro. *EMBO J* 2002;**21**:5899–910.

62. Mita P, Wudzinska A, Sun X, Andrade J, Nayak S, Kahler DJ, Badri S, LaCava J, Ueberheide B, Yun CY, et al. (2018). LINE-1 protein localization and functional dynamics during the cell cycle Elife 7.
63. Pampalona J, Frias C, Genesca A, Tusell L. Progressive telomere dysfunction causes cytokinesis failure and leads to the accumulation of polyploid cells. *PLoS Genet* 2012;**8** e1002679.
64. Goytisolo FA, Samper E, Edmonson S, Taccioli GE, Blasco MA. The absence of the dna-dependent protein kinase catalytic subunit in mice results in anaphase bridges and in increased telomeric fusions with normal telomere length and G-strand overhang. *Mol Cell Biol* 2001;**21**:3642–51.
65. Kanagasabai T, Venkatesan T, Natarajan U, Alobid S, Alhazzani K, Algahtani M. Regulation of cell cycle by MDM2 in prostate cancer cells through Aurora Kinase-B and p21WAF1(/CIP1) mediated pathways. *Cell Signal Rathinavelu A* 2019 109435.
66. Wagener R, Alexandrov LB, Montesinos-Rongen M, Schlesner M, Haake A, Drexler HG, Richter J, Bignell GR, McDermott U, Siebert R. Analysis of mutational signatures in exomes from B-cell lymphoma cell lines suggest APOBEC3 family members to be involved in the pathogenesis of primary effusion lymphoma. *Leukemia* 2015;**29**:1612–5.
67. Gu J, Chen Q, Xiao X, Ito F, Wolfe A, Chen XS. Biochemical Characterization of APOBEC3H Variants: Implications for Their HIV-1 Restriction Activity and mC Modification. *J Mol Biol* 2016;**428**:4626–38.
68. Starrett GJ, Luengas EM, McCann JL, Ebrahimi D, Temiz NA, Love RP, Feng MB, Adolph MB, Chelico L, Law EK, et al. The DNA cytosine deaminase APOBEC3H haplotype I likely contributes to breast and lung cancer mutagenesis. *Nat Commun* 2016;**7**:12918.
69. Renner TM, Belanger K, Goodwin LR, Campbell M, Langlois MA. Characterization of molecular attributes that influence LINE-1 restriction by all seven human APOBEC3 proteins. *Virology* 2018;**520**:127–36.
70. Porro A, Feuerhahn S, Reichenbach P, Lingner J. Molecular dissection of telomeric repeat-containing RNA biogenesis unveils the presence of distinct and multiple regulatory pathways. *Mol Cell Biol* 2010;**30**:4808–17.
71. Maicher A, Lockhart A, Luke B. Breaking new ground: digging into TERRA function. *Biochim Biophys Acta* 2014;**1839**:387–94.
72. Belancio VP, Whelton M, Deininger P. Requirements for polyadenylation at the 3' end of LINE-1 elements. *Gene* 2007;**390**:98–107.
73. Rodic N, Sharma R, Sharma R, Zampella J, Dai L, Taylor MS, Hruban RH, Iacobuzio-Donahue CA, Maitra A, Torbenson MS, et al. Long interspersed element-1 protein expression is a hallmark of many human cancers. *Am J Pathol* 2014;**184**:1280–6.
74. Lee E, Iskow R, Yang L, Gokcumen O, Haseley P, Luquette 3rd LJ, Lohr JG, Harris CC, Ding L, Wilson RK, et al. Landscape of somatic retrotransposition in human cancers. *Science* 2012;**337**:967–71.
75. Lawlor RT, Veronese N, Pea A, Nottegar A, Smith L, Pilati C, Demurtas J, Fassan M, Cheng L, Luchini C (2019). Alternative lengthening of telomeres (ALT) influences survival in soft tissue sarcomas: a systematic review with meta-analysis BMC Cancer 19, 232.
76. Elsasser SJ, Noh KM, Diaz N, Allis CD, Banaszynski LA. Histone H3.3 is required for endogenous retroviral element silencing in embryonic stem cells. *Nature* 2015;**522**:240–4.
77. Chen YA, Shen YL, Hsia HY, Tiang YP, Sung TL, Chen LY. Extrachromosomal telomere repeat DNA is linked to ALT development via cGAS-STING DNA sensing pathway. *Nat Struct Mol Biol* 2017;**24**:1124–31.
78. Kreilmeier T, Mejri D, Hauck M, Kleiter M, Holzmann K. Telomere transcripts target telomerase in human cancer cells. *Genes (Basel)* 2016;7.
79. Lafferty-Whyte K, Cairney CJ, Will MB, Serakinci N, Daidone MG, Zaffaroni A, Bilsland A, Keith WN. A gene expression signature classifying telomerase and ALT immortalization reveals an hTERT regulatory network and suggests a mesenchymal stem cell origin for ALT. *Oncogene* 2009;**28**:3765–74.
80. Jachowicz JW, Bing X, Pontabry J, Boskovic A, Rando OJ, Torres-Padilla ME. LINE-1 activation after fertilization regulates global chromatin accessibility in the early mouse embryo. *Nat Genet* 2017;**49**:1502–10.
81. De Cecco M, Ito T, Petrashen AP, Elias AE, Skvir NJ, Criscione SW, Caligiana G, Brocculi G, Adney EM, Boeke JD, et al. L1 drives IFN in senescent cells and promotes age-associated inflammation. *Nature* 2019;**566**:73–8.
82. Liu N, Lee CH, Swigut T, Grow E, Gu B, Bassik MC, Wysocka J (2018). Selective silencing of euchromatic L1s revealed by genome-wide screens for L1 regulators Nature 553, 228–232.